

NASA Technical Memorandum 102648


(NASA-TM-102648) NASA. LANGLEY RESEARCH
CENTER DRY POWDER TOWPREG SYSTEM (NASA)
50 p

N92-22639

G3/24 **Unclas**
0085739

LaRC DRY POWDER TOWPREG SYSTEM

Robert M. Baucom and Joseph M. Marchello

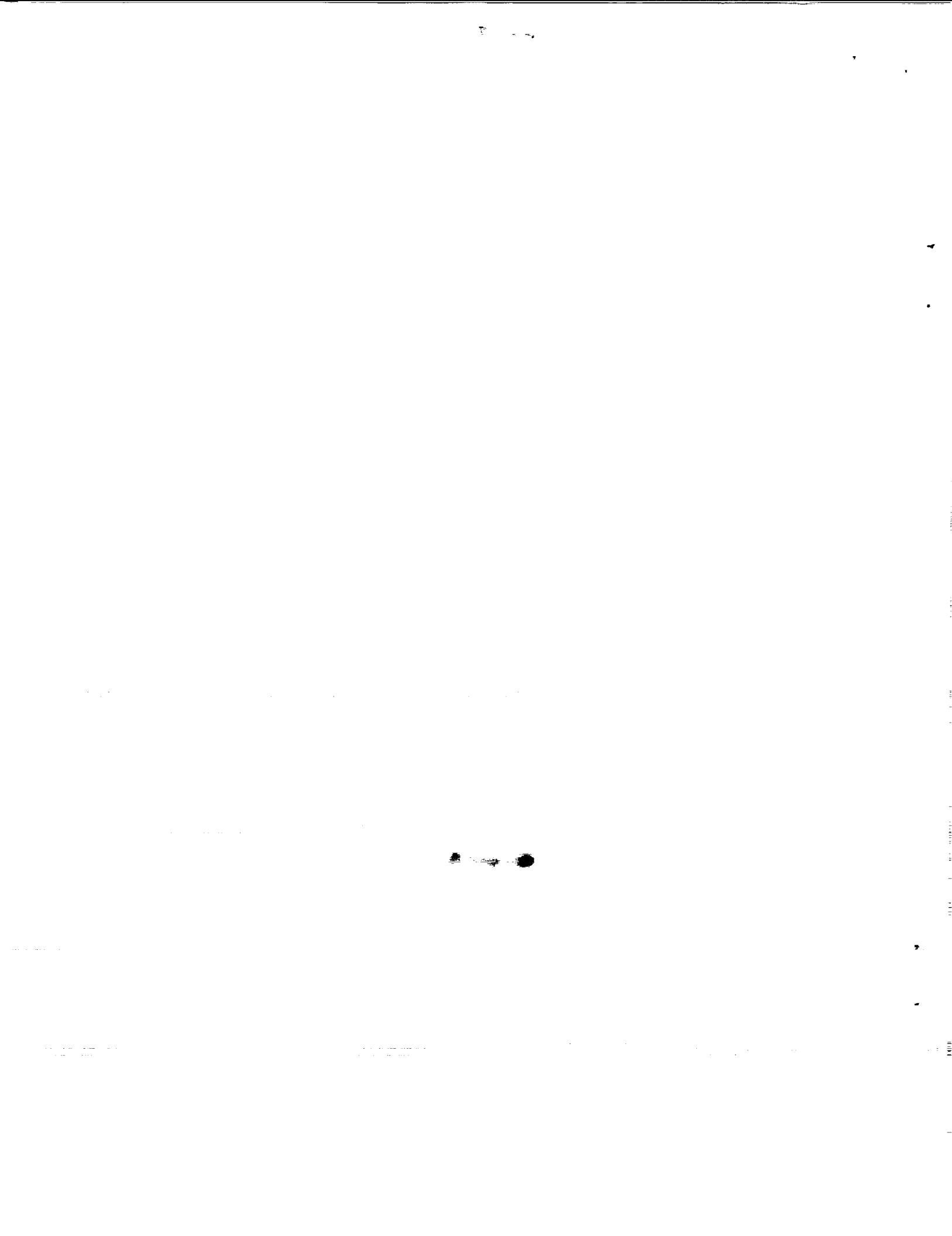

Date for general release April 30, 1992

APRIL 1990

NASA

National Aeronautics and
Space Administration

Langley Research Center
Hampton, Virginia 23665-5225



1.0 INTRODUCTION

Thermoplastic composites offer the potential of more attractive mechanical properties at elevated temperatures than do other materials. The primary concern in achieving this potential has been the difficulty experienced in combining thermoplastics with continuous fiber tows.

The high viscosity of the polymer melts and the limited solubility of the polymer in volatile solvents have ruled out conventional hot melt and solution prepregging methods. This in turn has led to efforts to develop other combining methods such as emulsion, slurry and dry powder (1). Among these, dry powder prepregging appears to be the more promising approach (2).

The dry powder prepreg processes under development contact the tow with powder and either encase, bind or sinter the powder to the fibers (3,4). Because of the tendency for movement of powder encased with the tow in an extruded tube, and for binder failure with powder loss during weaving, sintering appears to be the preferred method for attaching the powder.

The dry processes spread the tow and contact it with powder suspended in air or nitrogen. Investigators at Georgia Institute of Technology and the University of Akron utilize electrostatic force to enhance the deposition of the particles on the tow. At Clemson University (5) and NASA Langley Research Center, LaRC, the powder contacts the tow in fluidized beds.

The purpose of this memorandum is to report on dry powder towpreg process development at LaRC. The primary objective of the experimental and theoretical work was to obtain design and performance data and to develop scale up information for the fluidized bed process.

One goal of this study has been to weave the powder impregnated tow into two-dimensional preforms. For many thermoplastic polymers, this approach is an

attractive alternative to resin-transfer molding where the high melt viscosity of the polymer often prevents complete impregnation of the woven substrate. To successfully weave towpreg requires that it have appropriate powder-fiber fusion and flexibility.

2.0 EXPERIMENTAL

2.1 Starting Materials

Unsize Hercules AS-4 carbon fibers in 3K and 12K tows were used with four matrix polymer powders: LARC-TPI 2000, having an average diameter of 7 micrometers, and LARC-TPI 1500, having an average diameter of 19 micrometers, obtained from Mitsui Toatsu Chemical, Inc.; PEEK 150 having an average diameter of 17 micrometers, obtained from ICI Fiberite and ground by BASF; and PMR 15, having an average diameter of 1.5 micrometers, obtained from Dexter-Hysol Aerospace, Inc.

2.2 Towpreg System

The experimental system was composed in sequence of: the tow feed spool with tow tension brake; the fluidization chamber with powder feeder; the electric oven; the quality control monitor; and, the take-up spool with tow speed control, Figure 1.

2.3 Tow Tension

Because tow tension is important to the performance of the pneumatic tow spreader, a feed spool brake system was used to set and maintain tow tension during prepreg runs. A spring loaded graphite pad brake was mounted to the end of the roller. Pressure on the brake surface is achieved by tightening a wing nut on the screw that passes through the spring coil to the pad.

The tow tension brake was calibrated for different wing nut settings by determining the amount of weight hung on the tow that first caused the spool to rotate. The unbraked spool was mounted on air bearings and turned freely with less than a four grams resistance. Brake friction consists of two parts, the inertia required to set the spool in motion and the sliding friction once it is moving.

Since the unbraked turning inertia was small, it was assumed the tow tension that would be in effect during the operation of the prepreg unit was the sliding brake value. The brake was calibrated in increments up to 75 grams (2.6 oz.) of tow tension at 3 complete wing nut turns. Repeated tests indicated that tow tension could be set and maintained within 10 percent.

2.4 Pneumatic Spreader

The tow bundle entered the spreader at the throat of a flat expansion section. Air entered at the tow outlet slot and was drawn through holes in the side walls of the expansion section into a vacuum manifold. This crossflow of air provided drag on the carbon fibers resulting in tow spread across the flat channel.

The tow expansion section was 0.624 cm (0.25 in.) high and 43.8 cm (17.5 in.) long and the exit slot was 0.22 cm (0.090 in.) high, 1.6 cm high and 5.08 cm (2 in.) wide for the 12K tow. With 3K tow the section height was reduced to 0.31 cm (0.125 in.) and the exit slot height to 0.1 cm (0.040 in.). The tow spread angle from the entrance throat to the outer edge of the exit slot was 6 degrees. To minimize problems with loose fibers being drawn into the sidewall holes, the sidewall angle from the throat was 8 degrees. Nine holes were located along each sidewall with diameters of 0.20, 0.23, 0.27, 0.31, 0.35, 0.39, 0.43, and 0.47 cm (0.080, 0.094, 0.109, 0.125, 0.141, 0.156, 0.172 and 0.187 in.).

Control of the pressure drop for flow through these holes, together with tow tension adjustments determined the tow spread for angles up to 6 degrees or a 5.08 cm (2 in.) width of 12K tow. With 3K tow the spread width was 1.87 cm (0.75 in.). A

series of calibration runs were made to correlate the range of tow brake settings 0 to 75 grams (0 to 2.6 oz.) and vacuum levels 0 to 3 kPa (0 to 0.50 psi) with tow spread angle for tow rates up to 50 cm/sec (100 ft/min) for this unit.

2.5 Particle Feeder

To sustain the powder cloud density in the deposition chamber resin powder must be fed to it at rates of the order of two gram per minute depending on the tow speed, prepreg level, and powder losses. Initially a bubbling bed feeder was used to supply powder to the chamber. It was replaced with a screw feeder for the extended duration runs during the last part of the study.

The bubbling bed feeder consisted of a vertical plexiglass tube 45 cm (18 in.) high with an inside diameter of 4.4 cm (1.75 in.). At the start of a prepreg run powder was added to bring the settled bed to about 20 cm (8 in.) below the exit tube at the top of the cylinder. During operation, when the settled bed level had decreased to 30 cm (12 in.) from the top, resin was added. Nitrogen was fed into two opposing bottom openings so that it caused vigorous bubbling in the resin bed with flow out the top opening of a uniform feed stream of resin suspended in nitrogen. Samples of the feed stream particle size distribution at intervals of operation showed no significant change. The vertical column bubbling bed column is, intentionally, a poor elutriation type particle separator (6,7).

A cartridge filter was used to calibrate the feed system. The procedures involved vacuum cleaning and weighing the cartridge filter, placing it in the feeder exit line, running the feeder for five minutes at a set nitrogen rate, and reweighing the cartridge to determine the weight of the powder collected. In this way data were obtained for the grams of resin per minute conveyed by the nitrogen flow measured in cubic feet per hour.

At a given nitrogen flow rate, R , the resin feed conveyed from the bubbling bed, F , changes with the amount of resin in the cylinder. That is, the resin flow

decreases with time, τ , of feeder operation as shown by the feeder calibration relationship: $F = (0.204R - 1.29)/(1 + 0.085 \tau)$. This expression covers nitrogen flow rates between 0.28 and 1.10 m³/hr. (10 and 40 ft³/hr.) for feeder operating times up to 45 minutes. To maintain a constant resin mass flow the nitrogen rate must be increased during the interval between refilling. For example, with $F = 2$ gm/min (0.07 oz./min): $R = 16.1 + 0.85 \tau$, the initial nitrogen rate is 0.46 m³/hr. (16.1 ft³/hr.) and after 20 minutes it should be 0.93 m³/hr. (33 ft³/hr) to sustain the desired 2 gm/min (0.07 oz./min) of resin flow.

The bubbling bed feeder, described above, performed well with LARC-TPI, but presented operating difficulties for PEEK and PMR powders which have poorer pourability and tend to cake. Because of these concerns, and because the feeder had limited capacity, it was replaced with a dry powder feeder, AccuRate Model 304/310, manufactured by AccuRate, Inc. of Whitewater, Wisconsin.

The AccuRate screw feeder has a special feature for uniformly delivering powder. Its bottom sloping walls are flexible vinyl and paddles are used to flex them every few seconds thereby shifting the powder downward into the screw. The unit is capable of handling many types of powders, including LARC, PEEK and PMR, over extended periods of operation, with flow rates as low as 0.2 g/min.

2.6 Fluidization Chamber

The fiber tow from the pneumatic spreader enters the fluidized bed unit through a narrow slot on one side, passes horizontally through three slotted baffles, enters the main chamber, then passes through three slotted baffles and a wall slot as it leaves the unit.

The central chamber is 15 cm (6 in.) long in the tow travel direction and 20 cm (8 in.) across. The rectangular portion is 10 cm (4 in.) high. The four sided pyramid bottom extends 11.25 cm (4.5 in.) down to the fan inlet. The walls of the pyramid are

18.75 cm (7.5 in.) long. The volume of the fluidization section, exclusive of fan and return lines, is 5600 cc (359 in³).

During the initial runs it was observed that flow generated electrostatic charge appeared to cause a significant amount of powder to adhere to the sloping Plexiglas walls. To alleviate this thin metal sheets were attached to the pyramid bottom sides of the chamber. These sheets were electrically grounded and served to permit static electricity to leak from the particles to ground. There was a marked reduction in powder accumulation on these surfaces in subsequent runs.

At the start of a prepreg run an initial amount of powder was placed in the chamber. Fresh powder and nitrogen from the feeder entered on one side in the early runs. In the later runs powder was fed at the top of the chamber using the screw feeder. A fan at the bottom of the chamber removed powder and nitrogen and blew it into external tubing which conveyed the mixture up to where it re-entered at the top of the chamber. This flow recirculation, about 0.03 m³/min (1.0 ft³/min), together with a vibrator against the chamber wall, served to keep the resin powder suspended.

The unit has three settling sections at the tow entrance and exit sides. The baffles that form these sections extend from the top to within 1.0 cm (0.4 in.) of the bottom. In these sections, powder settled out onto the sloped bottom and slide to the fan intake. When operating with the bubbling bed feeder, the nitrogen that conveyed feed to the unit was withdrawn at the top of the two outer settling chambers. The vacuum level drawn on the settling chambers was adjusted to keep powder from escaping through the tow slots.

The recirculation fan was driven by a motor beneath it. Powder has the tendency to leak into the fan shaft bearings resulting in fan operating problems. This was overcome by mounting the two shaft bearings in the ends of a cylinder and applying nitrogen pressure to the cylinder. The small nitrogen flow out through the

bearings served to keep resin from entering and greatly reduced maintenance requirements.

2.7 Electrostatic Deposition

Powder deposition also was carried out using an electrostatic fluidized bed coating unit manufactured by Electrostatic Technology, Inc. of New Haven, CT (2). Air, at flow rates up to 150 CFH, enters the bottom section of the unit and is given a negative charge, at applied voltages up to 75 kV, as it passes a wire mesh electrode. The air then flows up through a porous plate and into the fluidized powder section where some charge is transferred to the powder particles, and all charge is finally transferred to the grounded tow,

During these experiments the fluidization chamber, Section 2.6, was replaced with the electrostatic unit. The spread tow passes through slots in a Plexiglas box on top of the 6 x 6 inch porous plate. The box has trapezoidal ends rising 4 inches to a flat 4 x 6 inch top. The volume of the box is 2000 cc. The tow travel path length is six inches which is the same as that of the fluidized bed chamber. During operation a vacuum is drawn on an outlet in the top, next to the tow inlet, to remove the air and to keep powder from escaping through the tow slots. A baffle plate was positioned between the tow inlet and air outlet to reduce powder carryover.

2.8 Electric Oven

An electric oven, Type 21100 Tube Furnace manufactured by Thermodyne, Inc. of Dubuque, IA, with a 5 cm diameter and 37.5 cm long tubular core was used to heat the powder laden tow from the fluidization chamber. Because of the important role of oven temperature and residence time in powder fusion and tow flexibility the oven temperature axial profile and was measured. Data obtained from this calibration were as follows:

Position of Thermocouple (inches in from oven opening)	Oven Control Setting		
	550°F (288°C)	575°F 302°C)	600°F (316°C)
Thermocouple reading at each position, °F			
0	208	—	245
1	290	325	442
2	504	570	660/670
3	632/649	690	739
4	654	713	765/762
5	695	703	786
6	691	724	781
7	652	703	772
8	653	720	762

Using this data the calibration for the central portion* of the oven was obtained.

Oven Setting °C	Oven Temperature °C
250	274
290	355
300	375
310	395
320	415
350	475
400	580

*The center 13 inches of the overall 15 inch long tube furnace.

2.9 Resin Control Monitor

An instrument for on-line continuous monitoring of the towpreg resin content was developed in conjunction with Analytical Services and Materials, Inc. of Hampton, VA. Towpreg is composed of electrically conducting carbon fibers and dielectric polymer resin. The monitor measures the electric capacitance of the towpreg, which is a function of its resin content (8,9).

The monitor system is shown schematically in figure 2. Towpreg leaving the oven passes through a 23 cm (9 inch) long detector consisting of two condenser plates and an outer metal cylindrical shell. Teflon, or a similar insulator material, is used to hold the plates in the cylinder and to guide the towpreg through a central slot, 0.5 cm wide and 0.05 cm high. It also serves to insulate the towpreg, plates, and shell.

Clean tow, leaving the feed spool, passes over a metal bar grounded to the capacitance meter. A lead from the outer metal cylinder of the monitor also is grounded to the meter. This electrically isolates the system. A 20 V, 10 kHz signal is applied to the capacitor plates. The capacitance between the carbon fibers and the metal plates is measured and calibrated as a function of the amount of resin present. The system amplifier circuit provides an output signal voltage used to drive the takeup spool motor speed controller.

2.10 Loom

Towpreg was woven using a hand loom manufactured by Harrisville Designs, Inc. of Harrisville, NH. The device is a 22 inch high, eight harness, 10 treadle loom. Woven towpreg preform made with the loom was cut into 3 x 3 inch plies and stacked for compression molding.

3.0 DESIGN RELATIONS

3.1 Tow Spreader

In the pneumatic spreader tow fibers are subject to the tow tension, F_t , and the air drag, F_w , toward the wall. Under these forces a fiber would move at an angle, ϕ , given by

$$\text{Tan } \phi = F_w/F_t \quad (1)$$

Tow tension is set by the brake on the feed spool. Air drag on the fiber results from flow in the spreader chamber.

The air drag on a fiber can be determined from data correlations for flow passed a cylinder. The pressure difference between the air in the spreader and in the surrounding vacuum manifold is primarily due to the flow resistance of the small holes in the spreader section walls. For subsonic flow through these holes the air velocity, U_o , may be obtained from the orifice equation (6,7):

$$U_o = C_o (2g_c \Delta P / \rho)^{1/2} \quad (2)$$

Where C_o is the orifice coefficient, g_c the gravitational constant, ρ the air density and ΔP the pressure drop. The coefficient is constant, $C_o = 0.61$, in the flow range of interest.

In the spreader chamber, air flow toward the walls, U_w , is related to flow through the holes by the area ratio

$$U_w = U_o(A_o/A_w) \quad (3)$$

The air drag for flow passed a cylinder is (7)

$$F_w = C_D \rho U_w^2 D_f L / 2g_c \quad (4)$$

Where C_D is the drag coefficient, D_f the diameter and L the length of the fiber.

Substituting equations (2) and (3) into (4) gives

$$F_w = (C_D D_f L C_o^2 A_o^2 / A_w^2) \Delta P \quad (5)$$

with the exception of C_D all the terms in the bracket are constant. In the lower flow ranges the drag coefficient is a function of Reynolds number or U_w and may be expressed in terms of ΔP through equations (2) and (3). Therefore,

$$F_w = f(\Delta P) \quad (6)$$

and from equation (1) the fiber angle, ϕ , would be

$$\phi = \tan^{-1} [f(\Delta P)/F_t] \quad (7)$$

For a given tension, F_t , the angle can be set by the pressure difference drawn on the chamber. Conversely, for a given ΔP , the angle may be adjusted by changing the tow brake setting for the tension.

The above analysis has dealt with the air drag on a single isolated fiber. The tow is comprised of thousands of fibers and air flow passed a fiber is influenced by the surrounding fibers. While the exact flow conditions are unknown, the general form of equation (7) also would apply for a multifiber system. This suggests that the tow spread angle may be correlated as a function of tension and pressure drop.

3.2 Powder Deposition

The expanded fiber tow behaves like a fibrous filter. Particle collection is by momentum impaction, inception owing to van der Waals forces, Brownian diffusion and in some cases electrostatic force. Theoretical analysis (10) indicates the collection efficiency of a single fiber, η_o , is a function of the parameter, ψ ,

$$\psi = D_p^2 U \rho_p / 18 \mu D_f \quad (8)$$

Where D_p is the particle diameter, U , the gas velocity, ρ_p , the particle density, μ , the gas viscosity, and D_f , the fiber diameter.

The collection efficiency of a fiber when other fibers are nearby is given by the relationship (11):

$$\eta_{ii} = \eta_o [1 + 10 Re^{1/3} (1 - \epsilon_f)] \quad (9)$$

Where Re is the Reynolds number for flow passed the fiber and ϵ_f is the void fraction of the fiber mat.

The fiber-particle collision cross section is $[D_p + D_f]L$. For a particle cloud density, n , and gas velocity, U , the rate at which particles arrive at the fiber surface is $nU[D_p + D_f]L$. With an average collection efficiency, η_i , the rate of deposition on the N fibers in the tow is

$$dM/dt = n\eta_i U [D_p + D_f] L N \quad (10)$$

and

$$dM/dt = P W_t U_t / (1-P) \quad (11)$$

Where P is the weight percent resin in the tow prepreg, W_t , the clean tow weight per unit length and U_t , the linear tow rate. Combining equation (10) and (11) gives the resin-to-tow weight ratio:

$$P/(1-P) = \{ \eta_i U [D_p + D_f] L N / W_t \} n / U_t \quad (12)$$

For a given type of tow bundle, chamber dimensions and recirculation level, and resin powder, the term $\{ \}$ is constant. This is the transport operating equation for fluidized bed units. For a given system the prepreg level is directly proportional to the resin cloud density, n , and inversely proportional to the tow rate, U_t .

Particle collection efficiency is enhanced when the powder is fluidized by electrically charged air using the electrostatic unit, Section 2.7. The electric field increases the rate of charged particle migration toward the fibers and the particle-fiber collision cross section is increased due to the electric field.

Particle collection by electrostatic attraction is described by the Deutsch-Anderson equation (10,11):

$$\eta = 1 - \exp(-W_p L / U_t S) \quad (13)$$

where for particles impregnating a spread tow:

η = fractional collection efficiency

W_p = particle drift velocity, cm/sec

L = tow length in chamber, cm

U_t = tow rate, cm/sec

S = distance between porous plate and tow, cm

The particle drift velocity, W_p , is the rate at which charged particles migrate toward the surface of the electrically ground fibers. It is determined by a force balance between the viscous drag of the gas and the force of the electric field. The amount of charge transferred from the gas to the particles is the primary governing factor in determining the electric force on the particles and depends upon the particle size, gas composition, and mixing (11).

3.3 Cloud Density Limit

The powder recirculation capacity limitation of the system is an important design consideration for scale up because it sets the maximum resin cloud density. To provide a basis for system design an analysis of the flow characteristics of the system was conducted.

In operating the experimental unit it was found that the fan could not recirculate the powder when more than 150 grams of LARC-TPI 1500 powder was placed in the chamber. It also was observed that, when the fan stalled, the suspended powder in the external tube settled to a depth of 6 inches at the bottom of the tube. This information about the current system is used below to illustrate how the design correlations are applied.

3.3.1 Flow System

The fluidized bed towpreg unit is comprised of two different particle fluidization systems - upflow and downflow. In the external return tube gas flows up through the fluidized powder and conveys it to the top of the fluidized deposition chamber. The powder and gas flow into the chamber, pass through and around the spread tow with some powder being deposited on it, and flow down to the fan inlet at the bottom. The fan accelerates the particles and gas into the external tube to complete the flow cycle.

The flow characteristics of each section of the system may be analyzed using the conservation of energy equation for an adiabatic, incompressible, steady state flow process. The one-dimensional form of the equation, on a unit mass basis, is:

$$(1/g_c)UdU + (g/g_c)dh + dF + dW_s = 0 \quad (14)$$

which accounts for the kinetic, potential, and frictional energies, and work. Since the elevation change is small $g = g_c = 32.2 \text{ ft/sec}^2$. The equation may be integrated over different sections of the flow system to obtain the total energy analysis.

For the current system the values of various properties and dimensions are:

$$\rho_g = 0.075 \text{ lb/ft}^3, \rho_p = 95 \text{ lb/ft}^3$$

$$D_t = 0.083 \text{ ft}, L = 1.5 \text{ ft}, h = 1.0 \text{ ft},$$

$$\text{and } W_f = 1/18 \text{ Hp} = 30 \text{ ft-lb/sec.}$$

As the fan strains near its stalling point it generates its maximum delivery pressure and lowest volumetric flow rate. Because of their design, fans cannot generate a pressure increase of more than about 10 inches of water (0.36 psi) between their intake and outlet. Therefore, the energy analysis for flow conditions near or at the stalling point assumes the fan is delivering at its maximum pressure head.

3.3.2 Minimum Carrying Velocity

For upflow of gases and solids in vertical pipe, the maximum carrying velocity can be estimated using the correlation (7)

$$U_{g,m} = 910 (\rho_p / [\rho_p + 62.3]) D_p^{0.60} \quad (15)$$

where: $U_{g,m}$ is in ft/sec, ρ_p is the density of the solid particles in lb/ft^3 , and D_p is the particle diameter in ft.

Using equation (15) the minimum carrying velocities for different size particles are:

Particle Size		Minimum Carrying Velocity
microns	feet	ft/sec
10	0.0000833	1.96
20	0.000166	2.97
50	0.000417	5.16
100	0.000833	7.81

For the LARC-TPI 1500 used in the current system flow experiments, $D_p = 19$ microns so, the minimum gas velocity required to carry the particles up the external tube is about 3 ft/sec, which would be the flow rate at the point where the fan stalls and the flow system stops.

3.3.3 Flow System Pressure Losses

Total pressure drop for flow up a vertical pipe may be considered as the sum of that required to accelerate the gas and solids to the carrying velocity, friction between the flowing suspension and the pipe walls and between particles, and support of the gas and solids column (7). In addition, the external tube has smooth 90° bends at the bottom where it is attached to the fan outlet and at the top where it enters the deposition chamber. Beginning at the fan outlet the pressure losses for each section of the system in sequence are set forth in the following sections.

3.3.4 Acceleration

When operating near the stalling limit the gas and particles are accelerated to just above the minimum carrying velocity $U_{g,m} = U$ and

$$\Delta P_1 = (n_t + \rho_g)U^2/2g_c \quad (16a)$$

where ΔP_1 is in lb/ft² and n_t is the dispersed particle density in the external tube in lb/ft³.

For the current system $n_t \gg \rho_g$, $U = 3$ ft/sec, and

$$\Delta P_1 = n_t(3^2)/(2) (32.2) = 0.14 n_t \quad (16b)$$

3.3.5 Contraction

The suspension flows from the fan outlet into the tube with a reduction of the flow cross-sectional area. The pressure drop for flow contraction is

$$\Delta P_2 = K(n_t + \rho_g)U^2/2g_c \quad (17a)$$

where $K = 0.4(1.25 - S_2/S_1)$, S_2 is the tube area and S_1 is the fan outlet area.

For the current system the fan outlet is 2x2 inches and the tube is 1 inch in diameter. $S_2/S_1 = 0.785/4 = 0.196$ and $K = 0.42$, so that

$$\Delta P_2 = (0.42)n_t(3^2)/(2) (32.2) = 0.059 n_t \quad (17b)$$

3.3.6 Friction

For solids-to-gas weight rate ratios over 50 the sum of the pressure drops due to friction can be estimated using the correlation (7)

$$\Delta P_3 = 2.5L_e n_t U_s^{0.45} (D_p/D_t)^{0.25} \quad (18a)$$

where: L_e is the equivalent length of pipe, ft; n_t is the dispersed solids density, lb/ft³; D_p is the particle diameter, ft; and, D_t is the tube diameter, ft.

The solids flow slower than the gas. Solids flow slippage correlations for high particle loadings level off at the limit of one half the gas velocity,

$$U_s = U/2 \quad (18b)$$

Flow resistance due to smooth 90° bends may be expressed as 26 D_t of equivalent pipe length (7) so that for the two bends

$$L_e = L + (2) (26)D_t = L + 52D_t \quad (18c)$$

combining equations gives

$$\Delta P_3 = 2.5(L + 52D_t) (n_t + \rho_g) (U/2)^{0.45} (D_p/D_t)^{0.25} \quad (18d)$$

For the current system

$$\Delta P_3 = 2.5(1.5+52[0.083])n_t(3/2)^{0.45}(0.000166/0.083)^{0.25}$$

$$\Delta P_3 = 3.74 n_t \quad (18e)$$

3.3.7 Column

The vertical column pressure difference between that of the tube and the chamber is

$$\Delta P_4 = (n_t - n)h \quad (19a)$$

where n_t is the particle cloud density in the vertical tube and n the particle cloud density in the deposition chamber.

For the current system, $h = 1$ ft

$$\Delta P_4 = n_t - n \quad (19b)$$

3.3.8 Expansion

The suspension flows from the tube into the chamber with an expansion of the flow cross-sectional area. The pressure drop for flow area expansion is

$$\Delta P_5 = (n_t + \rho_g)(U^2/2g_c)(1 - S_1/S_2) \quad (20a)$$

For the current system the chamber area is much larger than the tube area, $S_1 \gg S_2$, and $n_t \gg \rho_g$ so that

$$\Delta P_5 = n_t(3^2)/(2) (32.2) = 0.14 n_t \quad (20b)$$

3.3.9 Downflow

Friction resistance for flow downward in the deposition chamber is assumed to be negligible compared to the other flow resistances.

3.3.10 Total Pressure Loss

The sum of the above pressure losses represents the system resistance to flow and is provided by the fan recirculation.

For the current system the total pressure drop is

$$\Delta P_T = 0.14n_t + 0.059n_t + 3.74n_t + n_t - n + 0.14n_t \quad (21a)$$

$$\Delta P_T = 5.08n_t - n \quad (21b)$$

Consideration of the magnitudes of the various terms indicates that flow friction in the pipe and support of the suspended column of solid particles make up over 90% of the pressure drop or work required of the fan.

The maximum pressure increase delivered by fans at the point where they cease to deliver due to excessive flow resistance is about 10 inches of water = 0.36 psi = 51 lb/ft². Assuming this is the case for the current system

$$\Delta P_T = 51 = 5.08n_t - n \quad (21c)$$

or

$$n_t = 10.03 + 0.202n \quad (21d)$$

3.3.11 Material Balance

The distribution of resin charged to the system, m_i , is

$$m_i = n_t V_t + n V_c \quad (22a)$$

where V_t is the tube volume and V_c the chamber volume.

For the current system, $V_c = 5600 \text{ cc} = 0.20 \text{ ft}_3$, and $V_t = (\pi/4)D_t^2 L = (0.785)(0.0833)^2 (1.5) = 0.0082 \text{ ft}_3$. Then

$$m_i = 0.0082n_t + 0.20n \quad (22b)$$

The fan stalls at $m_i = 150 \text{ g} = 0.33 \text{ lb}$ so that

$$m_i = 0.33 = 0.0082n_t + 0.20n \quad (22c)$$

and

$$n_t = 40.2 - 24.4n \quad (22d)$$

3.3.12 Maximum Cloud Density

Combining the total pressure drop relation for the current system at the flow stall condition (minimum carrying velocity), equation (21d), and the material balance with the amount of powder that just causes stalling (150 g), equation (22d), gives:

$$n = 1.23 \text{ lb/ft}_3 = 0.0197 \text{ g/cc}$$

$$n_t = 10.3 \text{ lb/ft}_3 = 0.164 \text{ g/cc}$$

The settled powder density of LARC-TPI is 0.516 g/cc and n_t is 0.164 g/cc or about one third the settled density. This value of n_t also is about equal to the lower limit of fluidization bed expansion (7). In those two regards the calculated value appears to be reasonable.

Another check on the predicted cloud density is the observed amount of powder in the external tube when flow stops due to stalling of the fan. The volume of the tube is $(0.785) (0.0833)^2 (1.5) = 0.00817 \text{ ft}^3$ and with $n_t = 10.3$ the amount of powder that settles out in the bottom of the tube at stall is $(10.3) (0.00817) = 0.0842 \text{ lb} = 38 \text{ g}$. For a settled powder density of 0.516 g/cc the powder volume is $(38)/(0.516) = 74 \text{ cc}$. The tube cross sectional area is $(0.785) (2.5)^2 = 4.9 \text{ cm}^2$ so that the settled powder depth would be $(74)/(4.9) = 15.5 \text{ cm} = 5.9 \text{ inches}$, which is the depth that has been observed in the tube when the system stalls.

3.3.13 Horsepower

The current system employs a centrifugal fan (squirrel cage) with backward-curved blades driven by a 3000 rpm, 1/18 horsepower (42 Watts) motor. Performance characteristics of such fans (7) show that they develop maximum output pressure at between 40 and 50% efficiency. The work done by the fan is

$$W_s = EW_f = Q(\Delta P_T) \quad (23a)$$

where W_f is the work required, E the fan efficiency, and Q is the volumetric flow rate, which must be adjusted for the density of the entering suspension. The linear velocity of gas in the tube is obtained by dividing the volumetric rate by the tube area so that

$$W_s = EW_f = [A_t U] (n/\rho_g) (\Delta P_T) \quad (23b)$$

For the current system at the stalling point the efficiency is

$$E = [(0.00543) (3) (1.23/0.075)] (51) (18/550) = 0.44$$

This calculated fan efficiency of 44% at stalling is consistent with fan performance correlations and provides another demonstration of the consistency of the analysis.

3.3.14 Particle Size

The stalling point is a function of the properties of the powder and dimensions of the system as brought out in the various correlations presented above.

If the powder charge that causes stalling is not known it may be predicted by including the fan horsepower relation in the analysis. To illustrate this procedure the following analysis was made for the maximum cloud density of a powder with an average particle size of 10 microns.

From Section 3.3.2 the minimum carrying velocity is 2 ft/sec and a from Sections 3.3.4 through 3.3.10:

$$\text{Acceleration} \quad \Delta P = n_t(2)^2/(2) (32.2) = 0.062n_t \quad (24a)$$

$$\text{Contraction} \quad \Delta P = (0.42)n_t(2)^2/(2) (32.2) = 0.026n_t \quad (24b)$$

$$\text{Friction} \quad \Delta P = 2.5[1.5+52(0.083)]n_t(2/2)^{0.45}(0.000083/0.083)^{0.25}$$

$$\text{and} \quad \Delta P = 2.58n_t \quad (24c)$$

$$\text{Column} \quad \Delta P = n_t - n \quad (24d)$$

$$\text{Expansion} \quad \Delta P = n_t(2)^2/(2) (32.2) = 0.062n_t \quad (24e)$$

Total pressure drop

$$\Delta P_T = 0.062n_t + 0.026n_t + 2.58n_t + n_t - n + 0.062n_t$$

$$\text{and} \quad \Delta P_T = 3.73n_t - n \quad (24f)$$

For the fan maximum pressure, $\Delta P_T = 51$, from equation (24f)

$$n_t = 13.67 + 0.268n \quad (24g)$$

From Section 3.3.11 the material balance is

$$m_i = 0.0082n_t - 0.20n \quad (22b)$$

In this case m_i is unknown, so that the above two equations have three unknowns: n_t , n and m_i . The third equation is from Section 3.3.13. For a fan efficiency of 44% from equation (23b) $(0.44) (550/18) = 13.5 = 0.00545(2) (n/0.075) (51)$ and

$$n = 1.82 \text{ lb/ft}^3 = 0.029 \text{ g/cc}$$

In the tube

$$n_t = 13.67 + (0.268) (1.82) = 14.1 \text{ lb/ft}^3 = 0.226 \text{ g/cc}$$

and the maximum amount of 10 micron powder the current system can handle is

$$m_i = 0.0082 (14.1) + 0.20 (1.82) = 0.446 \text{ lb} = 202 \text{ g}$$

The system should be capable of fluidizing up to about 200 grams of 10 micron powder. While stall tests were not made for 10 micron powder, the system did recirculate 200 grams of 7 micron powder in several experiments.

Similar calculations may be made for other particle sizes and different equipment sizes. This capability for determining the powder recirculation limit and the corresponding chamber powder cloud densities is particularly important in the design of commercial powder towpreg units.

3.3.15 Cloud Density

A knowledge of the chamber cloud density at a given set of operating conditions is needed for design purposes to use in determining the towpreg resin content from the deposition rate, equation (12).

The previous sections have dealt with the maximum amount of powder the system can handle just before it stalls. The relations presented above also may be used to determine the cloud density in the chamber for powder loads at any level below the stall point.

To illustrate this procedure, for cases where the powder charge is below the maximum, the following analysis was made for a 20 micron powder in the current system

$$\text{Acceleration} \quad \Delta P = n_t U^2 / (2) \quad (32.2) = 0.0160 U^2 n_t \quad (25a)$$

$$\text{Contraction} \quad \Delta P = 0.42 n_t U^2 / (2) \quad (32.2) = 0.0065 U^2 n_t \quad (25b)$$

$$\text{Friction} \quad \Delta P = 2.5 [1.5 + 52(0.083)] n_t (U/2)^{0.45} (0.000166/0.083)^{0.25}$$

$$\text{and} \quad \Delta P = 2.23 U^{0.45} n_t \quad (25c)$$

$$\text{Column} \quad \Delta P = n_t - n \quad (25d)$$

$$\text{Expansion} \quad \Delta P = 0.016 U^2 n_t \quad (25e)$$

Total pressure drop is the sum of the above. Fan pressure delivery is generally fairly constant, decreasing only a few percent from the maximum, over a wide range of

flow rates (7), so in the absence of an actual fan performance curve, it is assumed that from adding the above pressure differences

$$\Delta P_T = 51 = 0.0385U^2n_t + 2.25U^{0.45}n_t + n_t - n \quad (25f)$$

From Section 3.3.11 the material balance is

$$m_i = 0.0082n_t + 0.20n \quad (22b)$$

and from Section 3.3.13 for a fan efficiency of 44%, $(0.44) (550/18) = 13.5 = (0.00545)U(n/0.075)$ (51)

or $U = 3.64/n$ (25g)

substituting into equation (25f) and rearranging gives

$$51 = 0.51n_t n^{-2} + 4.02n_t n^{-0.45} + n_t - n \quad (25h)$$

Equation (25h) together with the material balance, equation (22b) may be solved for various amounts of powder in the system, m_i . The following table was prepared using these equations.

Amount of Powder		Chamber Particle Cloud Density	
grams	pounds	lb/cu. ft.	g/cc
25	0.055	0.19	0.0030
50	0.110	0.38	0.0061
75	0.165	0.57	0.0091
100	0.220	0.78	0.0125
150	0.330	1.23	0.0197

For the current system with the 20 micron LARC-TPI the chamber cloud density is 0.0197 g/cc near the stall point when the system contains 150 grams of powder. If 100 grams is charged to the system the chamber cloud density is 0.0125 g/cc as shown in the above table.

3.3.16 Fluidization Level

In this section the design correlations for fluidized powder flow systems were presented and their use illustrated for the current bench scale unit. These general design relations correlate chamber size, fan capacity, and particle cloud density for different particle properties and flow conditions.

The correlations can be used to calculate the maximum amount of powder that may be charged to a given chamber and the corresponding cloud density and fan stalling limit. Alternatively, if a given cloud density is desired, the correlations may be used to calculate the range of choices of chamber dimensions, powder charge, and fan capacity for the system.

3.4 Flexural Rigidity

The cantilever test for fabric stiffness, ASTM D1388 - 64, may be used to determine the flexural rigidity of towpreg (12,13). To measure the flexural rigidity, a sample of towpreg is placed on a horizontal surface and one end is then slid out off the surface so that it extends over the edge. Sliding is continued until the tip of the towpreg bends down to a point where it contacts another surface inclined at a 41.5° angle to the horizontal, figure 3. The flexural rigidity, G , is then calculated from

$$G = W(O/2)^3 \quad (26)$$

where O is the overhang length of the towpreg, cm, and W is its areal weight, mg/cm².

3.5 Quality Control

To produce commercial quantities of towpreg, it is necessary to operate the towpreg unit for extended periods of time at high speed while making towpreg of a desired quality. Thus, quality control during extended operation is an important consideration in the powder towpreg process.

3.5.1 Quality Criteria

Users will require the towpreg to have specified: resin-fiber composition; flexibility; and, powder-fiber fusion. In making towpreg the resin level is established during the fluidized powder deposition step which is followed by thermal treatment for powder-fiber fusion. Because flexibility decreases with increased fusion, the thermal treatment step must be balanced such that adequate fusion is obtained without making the towpreg too stiff.

Weaving experiments indicate that the towpreg used as fill material must have a flexural rigidity below 10,000 mg-cm so that it bends and follows the shuttle action without breaking. Towpreg used as beam material must have a flexural rigidity below 100,000 mg-cm so that it does not break during heddle and comb action, and it must bind together the fibers so that they do not come loose, resulting in material thinning and comb clogging. This last condition requires using resin fusion to bind the unidirectional tow fibers in the beam material.

3.5.2 System Variables

Deposition of powder on the tow depends on the powder cloud density and tow residence time in the chamber. Cloud density is achieved by placing an initial amount of powder in the chamber and using the fan to fluidize and recirculate it. The cloud density is maintained during unit operation by feeding powder to the chamber at a rate equal to the rate at which it leaves on the tow. The tow residence time is the chamber length divided by the tow speed.

For a deposition chamber of a given length, the operating variables that govern towpreg resin content are cloud density and tow speed. While for most systems tow speed may be varied over a wide range, cloud density is restricted by the capacity of the fan circulation system. Minimizing chamber size will likely be a design concern, especially for multi-tow units. To keep the chamber as small as

practical its design would be based on operating just below the fan stalling condition, Section 3.3.

Chamber selection establishes the chamber length, and fan capacity selection fixes the maximum amount of powder that can be in the chamber. The unit may be operated at cloud densities below the maximum, thereby providing for control of resin level through the initial charge, which is a startup condition, and the powder feed rate. Thus, tow speed and powder feed rate are the operating variables with which to control towpreg resin content.

Thermal treatment is carried out by passing the powder laden tow from the deposition chamber through an electric oven. Design selection establishes oven length so that tow speed and oven temperature are the design variables with which to control powder fusion and towpreg flexibility.

In summary, the principal design variables are: deposition chamber length, fan capacity (or initial powder charge), and oven length. The principal operating variables for quality control are: tow speed, powder feed rate, and oven temperature.

3.5.3 Process Control

Once the system design has been selected the operating variables are used to achieve towpreg quality control during production. The process outputs to be maintained, within certain setpoints, by the control system are towpreg resin content, powder fusion, and flexibility. During continuous operation, regulatory control over output disturbances is accomplished by adjusting the tow speed, powder feed rate, and oven temperature.

A continuous resin content monitor was developed for use in a feedback control loop, Section 2.9. Theoretical analysis and data correlations for the deposition process provide information about the functional relation between resin content, tow speed, and feed rate, Section 3.2. Because the tow passes through the

chamber in a few seconds, the response time constant for tow speed, as a control variable, is of the order of one second. On the other hand, powder feed rates are a few grams per minute into a chamber containing over 100 grams of fluidized powder, making the response time constant of the order of several minutes. Thus, tow speed change offers a means of achieving adjustment to output disturbances in a matter of seconds, while the adjustment resulting from feed rate change would take much longer.

A two loop multivariable feedback control system would seem to be appropriate for resin content control. The system could use the signal from the resin content monitor to adjust the tow speed and powder feed rate. However, because both control variables would be activated by the signal from the resin monitor, there would be interaction between the two loops resulting in an unstable, or at least a poorly controlled system (14). In view of the potential for unstable operation, the two interacting loop system was dropped from consideration in favor of simply setting the feed rate at the level needed to maintain cloud density and using the tow speed alone to control towpreg resin content.

The correlation of particle fusion and towpreg flexibility to tow rate and oven temperature has been determined by experiment. Because of the nature of these properties, no continuous monitoring system has been developed for use in process quality control. The thermal treatment response time constants are similar to those of powder deposition. The tow passes through the oven in a few seconds, whereas changes in oven temperature require several minutes. Since tow speed is used to control resin content, it will be fairly constant, changing only enough to keep resin content between its set points. In view of these considerations, it was decided simply to control the oven temperature at the level, as indicated by data correlation, needed to produce the desired fusion and flexibility.

3.5.4 Control System

As described above, the towpreg process control is comprised of three single loop feedback systems. Prior to startup, the towpreg product quality requirements for resin content, flexibility, and powder fusion are used, with data correlations, to establish initial resin charge, powder feed rate, oven temperature, and tow rate. Powder is added to the chamber, the oven brought up to temperature, and the operation started.

During the steady continuous operation of the towpreg unit, powder feed rate and oven temperature are maintained within control set points using the feeder and oven controls provided by the equipment manufacturer. The resin content monitor signal is used to adjust the speed of the takeup spool drive motor. In this way the tow residence time in the chamber is adjusted to maintain towpreg resin content within the monitor set point range, e.g. 1 wt %.

4.0 RESULTS AND DISCUSSION

The bench scale dry towpreg system was operated over a wide range of conditions to confirm design theory and operating correlations for each component and thereby provide the basis for scale up to produce commercial quantities of towpreg.

4.1 Spreader Performance

The pneumatic tow spreader operated reliably with both 3K and 12K tows over extended periods of tow speeds as high as 50 cm/sec. The only operating concern occurred in instances where the tow broke, or the system was shutdown suddenly, such that loose fibers were drawn into the holes along the spreader sides. This required disassembling the unit and removing the fibers.

Comparison of tow spread angle calibration, as a function of tow tension and vacuum pressure, with the single fiber force balance calculations, Section 3.1, indicates that the tow spread angle is less than the theoretical single fiber angle (15). This is to be expected because the theory does not account for the effect of adjacent fibers and for air flow bypassing the tow fibers.

4.2 Powder Deposition

Operating experience with the fluidized bed and electrostatic units served to define the range of conditions for which acceptable towpreg could be made. This information was used to improve system design and operation and to prepare data correlations for system scale up.

4.2.1 Fluidized Powder Deposition

As discussed in Section 3.2, fluidized powder deposition design relationships may be based upon fibrous filter theory (15). Average particle sizes for the powders studied were from $D_p = 1.5 \times 10^{-4}$ cm for PMR-15 to $D_p = 19 \times 10^{-4}$ cm for LARC-TPI 1500. In the fluidization chamber $U = 1.5$ cm/sec, $\rho_p = 1.5$ g/cc, $\mu = 0.00187$ g/cm sec, and $D_f = 6 \times 10^{-4}$ cm. Therefore the single fiber collection parameter values ranged from $\psi = 0.0025$ for PMR-15 to $\psi = 0.40$ for LARC-TPI 1500.

Over this parameter range, the isolated fiber efficiency, η_o , is in the flat region of the correlation curve (9) with a theoretical value of $\eta_o = 0.0045$, Figure 4. The Reynolds number for flow passed the fiber is $Re = D_f U \rho_g / \mu = 0.00129$ and for a tow void fraction of 0.97 the collection efficiency of the average fiber, equation (9), is $\eta_i = 0.00465$.

The level of powder deposition on the tow as it passes through the chamber is

$$(P/[1-P]) = \{\eta_i U [D_p + D_f] (N/W_t)\} (L_n/U_t) \quad (12)$$

where the tow residence time is $\theta_c = L/U_t$.

For 6 micron carbon fibers $(N/W_t) = 1.43 \times 10^6$ cm/g, (3K tow weighs 0.0021 g/cm and 12K tow weighs 0.0084 g/cm). In the experimental chamber average fiber collection efficiency $\eta_i = 0.00465$ and the average gas flow rate $U = 1.50$ cm/sec.

Substituting gives

$$(P/[1-P]) = [D_p + D_f] \theta_c n \quad (27)$$

where θ_c is in seconds, n in g/cc and D_p and D_f are in microns.

Operating data over a range of conditions are given in Table 1. The last column presents the term $\{P/[1-P] (D_p + D_f) \theta_c n\}$, which according to Equation (27) should be equal to one. The average of this term for the 26 sets of operating data is 0.997 demonstrating the appropriateness of the powder deposition relationship for process design. As shown in Figure 5, the data scatter appears random and due primarily to errors of measurement.

As indicated in Table 1, the experimental data for powder deposition cover a wide range of operating conditions for the four powders. The procedures set forth in Section 3.3.15 were used with the initial amount of powder to determine the powder cloud densities. The applicability of Equation 27 is clearly demonstrated in regard to particle size. The 1.5 micron PMR-15 data and the 19 micron LARC-TPI 1500 are correlated together by the particle-fiber collision cross section term, as are data for the intermediate size powders.

The powder deposition relationship, Equation 12, may be expressed in several useful forms. For example, $(N/W_t) = 1.43 \times 10^6$ cm/g for all 6 micron carbon fiber tows, and $\eta_i = 0.00465$ for a wide range of chamber flow conditions, substituting

$$p = (P/[1-P]) = 0.665[D_p + D_f]ULn/U_t \quad (27a)$$

where p is the resin-to-fiber weight ratio, D_p and D_f are expressed in microns, U and U_t in cm/sec, and n in g/cc.

Further the linear gas flow rate in the chamber, U , may be replaced by the gas volumetric recirculation rate, Q , divided by the chamber area, Lw_c , $U = Q/Lw_c$ and with $D_f = 6$

$$p = 0.665[D_p + 6]Qn/U_t w_c \quad (27b)$$

where Q is in cc/sec and the chamber width, w_c , is in cm.

or

$$p = 0.665[D_p + 6]Q \theta_c n / L w_c \quad (27c)$$

Equation 27c is useful in scale up as it relates: chamber length, L , and width, w_c ; volumetric gas recirculation rate, Q ; tow residence time, θ_c ; powder cloud density, n ; and particle size, D_p , to resin deposition.

In working with a single powder, given chamber length and gas recirculation velocity the relationship may be expressed more simply. For example (15), LARC-TPI 2000 with $D_p = 7$ microns, $U = 1.5$ cm/sec and $L = 15$ cm for which one obtains:

$$p = 195 n / U_t \quad (27d)$$

The relationship between cloud density and tow rate, Equation 27d, establishes the resin quality control feedback response, Section 3.5

4.2.2 Electrostatic Deposition

The rationale for exploring electrostatic deposition of resin on tow arose from experience with electrostatic dry powder painting in which polyester and epoxy powders are deposited on metallic substrates. In the process the powder is metered into a compressed-air-driven spray gun and sprayed at the surface. An electrode in the gun ionizes the air and powder suspension. Charged powder is electrically attracted to the grounded surface. The coating is then fused and cured in an oven. The powder overspray is collected in air filters for reuse so that powder uses of 90 - 99% are possible (16). For heavy coatings, and to eliminate manual operation, fluidized units have been developed (12,17).

Electrostatic towpreg data using the Electrostatic unit, Sections 2.7 and 3.2, are presented in Table 2. The data are for a series of runs made to examine effects of ionizer air flow, discharge voltage, and tow speed.

Air enters the bottom of the unit and is given a negative charge, it then flows up through a porous plate and into the fluidization section where some charge is transferred to particles and all charge is finally transferred to the grounded tow. As shown in Table 2, with 12K tow the towpreg levels were at 7% for an air rate of 50 CFH and increased to 35% with air at 100CFH. A two-fold increase in towpreg level was obtained for 3K tow in going from 100CFH to 150CFH. These results indicate that the unit should be operated at its maximum (150CFH) air rate.

Test with 12K tow showed a towpreg level of 15% with no applied voltage and increased to 35% when 75 kV was applied. Similar results were obtained with 3K tow in that 18% was deposited with no voltage and 29% when 75 kV was applied. Powder deposition in the chamber of the Electrostatic unit increases sharply as applied voltage approaches 75 kV and is nearly double that when lower or no voltage is applied. These results indicate that the unit should be operated at or near its maximum (79 kV) voltage.

The inverse relationship between tow rate and prepreg level found for the fluidized bed also applies for the Electrostatic unit. That is, doubling the tow rate reduces the prepreg level by about 50% when all other variables are constant. The towpreg level is directly dependent on tow residence time for constant powder cloud density. At an ionizer air rate of 150CFH and an applied voltage of 75 kV, the data correlate in the form

$$p = P/[1-P] = 302 n/U_t \quad (27e)$$

Comparison of Equations 27d and 27e indicates that electrostatic deposition enhances powder deposition by about 50%. As indicated by examination of the terms in Equations 12 and 13, the increased powder deposition is due primarily to

the increase in particle-fiber collision cross section resulting from the electric field and to the higher gas flow rate in the chamber.

For powders with high electrical resistivity, gas conditioning using polar and ionic vapors can increase particle collection (10,13). A run was made in which water vapor was fed to the unit. The ionizer air rate was at 150CFH and 75 kV was applied. A 5CFH nitrogen feed stream was bubbled through 168°F water and mixed with the powder feed stream providing a 1.2 vol % moisture level in the gas. When operating dry without water vapor the towpreg level was 23%. With water vapor the towpreg level increased to 35%. Thus, gas conditioning can be used to enhance charge transfer to the particles and increase powder deposition.

4.3 Powder Material Balance

The powder material balance is an important consideration in design and scale up of the towpreg system. Powder is placed in the chamber at startup and is fed to the chamber during operation to maintain the powder cloud density. Powder leaves on the tow and with the gas flow to the vacuum system, Sections 2.6 and 2.7. Powder loss through the tow slots is reduced by the settling sections and baffles, and is essentially eliminated by adjusting the vacuum so that no powder is observed escaping from the tow slots.

During several runs powder samples were collected on a cartridge filter for material balance determination. These were steady state runs in which the powder level in the unit was constant and powder fed to the chamber either left on the tow as prepreg or was carried over with the gas. From the collected powder weight and the collection time the powder carryover was determined for these runs.

For the fluidized bed, with the bubbling bed feeder, the nitrogen feed conveying gas, at rates up to 40CFH, had to be removed by the vacuum to avoid flow out the slots. The material balance data indicated that between 15 and 20% of the powder fed was carried over with the nitrogen.

Using the screw feeder with the fluidized bed unit required only that the vacuum be sufficient to curtail the flow of air entrained by the tow as it passed out the exit slot. Consequently powder carryover was very low, generally less than one percent.

For the Electrostatic unit the air flow is once-through, at rates up to 150CFH. Tests indicated that powder carryover was as much as nine times that deposited on the tow. Chamber design changes, such as different baffle and settling chamber arrangements, can be used to reduce carryover, and powder can be collected and reused. However, the requirement for collection and reuse of significant amounts of carried over powder will be a concern of further development of the process.

4.4 Fusion and Flexibility

Towpreg flexibility and powder-fiber fusion are important for weaving and molding applications. These properties of the towpreg depend upon the temperature of the oven and the time that the powder laden tow takes to travel through the oven.

Flexural rigidity data are presented in Table 3 for towpreg having a range of resin content and fused at several different oven temperatures and residences times. The standardized cantilever test, ASTM D 1388-64, discussed in Section 3.4, was used to determine the flexural rigidity of towpreg samples.

As pointed out in Section 2.8, the oven temperature has a parabolic profile along the length. The temperature reported in Table 3 is the maximum oven temperature which is located in the central portion of the oven. The 3K tow was spread to between 15 and 20 mm during powder deposition and then allowed to contract to an average width of 5 mm as it passed through the oven. The areal weight of towpreg and, thus, the flexural rigidity were calculated based on a constant towpreg width of 5 mm.

Table 4 presents the flexibility data in a matrix display and summarizes the data by averaging the replicated samples. Examination of Table 4 shows that towpreg rigidity increases with resin content, and with oven temperature and residence time.

As indicated in Table 3, visual examination showed that for two samples the powder was not adequately fused to the fiber. These were processed at low temperature and high tow speed and had low flexural rigidity. They were acceptable in terms of flexibility, but unacceptable in terms of powder fusion, which points to the need to balance fusion and flexibility considerations in heat treating the towpreg.

As discussed in Section 3.5, the in-line sequential nature of the powder deposition and fusion processes places restrictions on the range of system operating conditions and resulting towpreg properties. The length of the powder deposition chamber and the power of the recirculating fan establish the upper limit on the tow rate at which a given resin level may be obtained. With this tow rate restriction and for a given oven length, the oven temperature is the only variable for fusion and flexibility control. This coupling of the deposition and fusion processes through the tow rate is reflected in the data presented in Tables 3 and 4 and should be taken into account in system design and scale up.

Scanning electron micrographs, SEM, were taken of various samples of towpreg to attempt to study the mechanisms that may govern the flexural properties of the resin-laden tow. SEM photographs indicate various levels of powder melting, fiber fusion, and melt flow along the length of the fibers. In general, it was found that higher oven temperatures, which produce significant polymer melting and wicking along the fibers, result in boardy towpreg. Wicking of the polymer melt creates extended regions of fiber-fiber fusion that reduce tow flexibility. By contrast, lower

temperatures promote partial fusion of the particles to the fibers without significant fiber-fiber fusion and flexibility can be maintained.

From the SEM photos, a great deal of variation was observed within each sample and from sample to sample. As shown in Table 3, overhang lengths range from 15 to 60 cm while SEM focuses on a small area of towpreg. That is, G is an integral or average value over many centimeters of material and the SEM details micrometer information. In view of the rather wide variation between SEM samples it probably would require a large number to obtain a composite microscopic picture that correlates with the macroscopic rigidity properties. Thus, the SEM photos primarily provided a qualitative view of the towpreg.

To examine the effect of the heat treatment step on melting during the powder coating process, differential scanning calorimetry measurements, DSC, were performed on samples of towpreg and on the neat resin. DSC scans for the LARC-TPI 1500 powder as received showed no T_g , only a T_m at 302°C. Reheating gives a T_g at 238°C and no T_m . For the as received powder, during the DSC, as the temperature increases the first indication of melting occurs at 280°C and the last at 320°C. The latent heat of melting is 34.8 J/g or 8.32 cal/g. The towpreg samples showed only the T_g at 238°C indicating that even at the shortest oven residence times, if fusion occurred, the as received crystallinity was removed in the heating process.

4.5 Weaving and Molding

Test specimens of both unidirectional fiber towpreg and woven towpreg were prepared and molded for testing. Unidirectional fiber applications utilize towpreg in filament winding or when prepared as multi-tow prepreg. Preform applications use towpreg in weaving and braiding operations.

Shear and flexure test specimens were prepared from the unidirectional towpreg of LARC-TPI 2000 on 12K tow carbon fibers produced using the fluidized

bed. Molding temperature was 15 minutes at 450°F and 1.0 hours at 660°F. Molding pressure of 5.5 MPa (800 psi) was applied starting on the rise to 660°F. Six short beam shear samples were cut from a specimen with 33.5 wt % resin and a virtually transparent C-scan. They gave an average short beam shear strength of 85.0 MPa (12.3 ksi) with a standard deviation of 0.9 MPa (1.3 ksi). Four flexure test samples were cut from another specimen with 32.5 wt % resin. The average flexure strength was 2228 MPa (323 ksi) with a standard deviation of 97.2 MPa (14.1 ksi). The average flexure modulus was 13.4×10^4 MPa (19.4 Msi) and the average deflection was 0.19%.

The hand loom, Section 2.10, was used to determine the flexibility requirements for weaving towpreg made from AS-4 fiber and LARC-TPI 1500 resin. Two dimensional 1,3 twill fabric preforms were successfully woven using towpreg of different composition and flexibility in the fill and beam directions. The first woven sample was prepared using 3K towpreg with 33% resin and $G = 67,000$ mg-cm beam material and 3K towpreg with 19% resin and $G = 3,000$ mg-cm as fill material.

Flexure test specimens were prepared from woven material made with LARC-TPI 1500 powder using 3K AS-4 tow (44 wt % resin, $G = 73,000$ mg-cm) as the beam material and 12K AS-4 tow (23 wt %, $G = 7,700$ mg-cm) as the fill material. Eight plies, each consisting of fifty 3K tows in the beam direction and fourteen 12K tows in the fill direction, were used for the molding specimens. Consolidation was at a temperature of 700°F and pressure of 300 psi. The six flexure test specimens were 29 wt % resin and gave a virtually transparent C-scan. The three beam samples had an average flexure strength of 134 ksi with a standard deviation of 3.5 ksi. The average flexure modulus was 8.1 Msi and the average deflection was 1.85%. The three fill samples had an average flexure strength of 83 ksi with a standard deviation of 4.0 ksi. The average flexure modulus was 5.7 Msi and the average deflection was 1.5%.

As pointed out in Section 3.5.1, the fill material must be sufficiently flexible that it can follow the shuttle action. Weaving tests indicate this requires that the flexural rigidity, $G < 10,000$ mg-cm. Beam material must not fail under the action of the hettle and comb and must bind the unidirectional fiber such that they do not clog the comb. This generally requires that $G < 100,000$ mg-cm. The combination must produce a woven material having an average resin content of about 32 wt %.

While it may be possible to meet all these requirements with one towpreg, experience weaving LARC-TPI towpreg led to the practice of making low resin content (25 wt %) towpreg for use as fill material, and high resin content (45 wt %) towpreg for use as beam material. This combination was successfully woven and molded into composite material.

5. CONCLUDING REMARKS

Fluidized beds offer a viable means of preparing tow prepreg from powder resin. Operating and design parameters for deposition of polymer powders on carbon fiber tows have been identified and used to explain bench scale experimental results. This information provides the basis for designing and building systems to operate at the commercial level.

In the fluidized bed unit gas and powder are continuously recirculated, whereas in the electrostatic unit air flow is once-through resulting in significant powder carryover. The greater equipment and operating requirements of the electrostatic process do not appear to justify the benefit of enhanced powder deposition.

The towpreg prepared using the LARC fluidized bed system may be used in weaving, filament winding and molding applications. Both unidirectional and woven molded test specimens made with the towpreg had good flexure and shear

properties. By controlling oven temperature and residence time, flexible towpreg with appropriate weaving properties may be produced.

6.0 ACKNOWLEDGEMENT

The authors gratefully acknowledge the assistance of Mr. John Snoha in constructing and operating the fluidized bed system, and Dr. Douglas Hirt for obtaining SEM and DSC data. They also greatly appreciate the advice and suggestion of Dr. Terry St. Clair, Dr. Norman Johnston and Dr. Hirt.

7.0 LITERATURE CITED

1. Babu Varughese and John Muzzy, "Combining LARC-TPI and Powder with Carbon Fiber by Electrostatic Fluidized Bed Coating," 21st International SAMPE Technical Conference, Atlantic City, September 1989.
2. John Muzzy, Babu Varughese, Vivan Thammonghol and Wayne Tincher, "Electrostatic Prepregging of Thermoplastic Matrices," 34th International SAMPE Symposium, pp. 1940-1051, May 1989.
3. J. L. Throne, R. M. Baucom, and J. M. Marchello, "Recent Developments in Dry Powder Prepregging on Carbon Fiber Tow," FiberTex Conference, Clemson University, October 1989.
4. K. Friedreich, T. Gogera and S. Fakirov, Composite Science and Technology, Vol. 33, pp. 97-120, 1988.
5. D. D. Edie, G. C. Lickfield, M.J. Drews, M. S. Ellison, L. E. Allen, J. R. McCollum and H. L. Thomas, "Thermoplastic Coating of Carbon Fibers," Annual Report 1987-1988, Advanced Engineering Fibers Laboratory, Clemson University.

6. J. M. Coulson and J. F. Richardson, Chemical Engineering, Vol. II, 2nd Edition, pp. 212, 682, 692, Pergamon Press, 1985.
7. J. H. Perry, Ed., Chemical Engineer's Handbook, 5th Edition, pp. 8-27, 5-45 to 46, 6-19 to 21, McGraw-Hill Book Co., 1981.
8. W. Michaeli and G. Burkhardt, "Dielectric Sensors for Low-Cost Cure Control," 34th International SAMPE Symposium Conference, p. 32-42, May 8-11, 1989.
9. David R. Day and David D. Shepard, "Thermoset Process Control Endpoint Determination with Dielectric Sensors," 21st International SAMPE Technical Conference, p. 1-6, September 25-28, 1989.
10. A. C. Stern, Ed., Air Pollution, 3rd Edition, p. 164-171, Academic Press, 1977.
11. J. M. Marchello, Control of Air Pollution Sources, pp. 49, 135, 150-154, 161-180, Marcel Dekker Publishers, 1976.
12. J. Muzzy, B. Varughese, V. Thammongkol and W. Tincher, "Electrostatic Prepregging of Thermoplastic Matrices, SAMPE J., 25, 15, 1989.
13. J. Muzzy, B. Varughese and P. H. Yang, "Flexible Towpreg by Powder Fusion Coating of Filaments," 1990 SPE ANTEC Proceedings, May 1990.
14. Jay Matley, Ed., Practical Process Instrumentation and Control, Vol. II, p. 4-9, McGraw-Hill Co., 1986.
15. R. M. Baucom and J. M. Marchello, "LaRC Powder Prepreg System," 35th International SAMPE Symposium, April 1990.
16. T. E. Higgins, Hazardous Waste Minimumization Handbook, p. 119-122, Lewis Publishers, Inc., 1989.
17. J. L. Throne and M. S. Sohn, "Electrostatic Dry Powder Prepregging of Carbon Fiber," 35th International SAMPE Symposium, April 1990.

Table 1

Powder Deposition Data on 3K AS-4 Carbon Fiber Tows

Weight Percent Powder on Tow, P	Chamber Residence Time, Seconds, θ_c	Chamber Powder Cloud, g/cc, n	Powder to Fiber Weight Ratio P/[1-P]	P/[1-P] ($D_p + D_f$) $\theta_c n$, θ_c in sec, n in g/cc, D_p and D_f in Microns
<u>LARC-TPI 2000. $D_p = 7$</u>				
46	3.6	0.020	0.85	0.91
41	3.6	0.014	0.70	1.07
34	3.6	0.0107	0.51	1.02
28	3.6	0.0071	0.39	1.17
<u>LARC-TPI 1500. $D_p = 19$</u>				
33	1.24	0.020	0.49	0.79
35	1.24	0.020	0.54	0.87
37	1.24	0.020	0.59	0.95
39	1.72	0.020	0.64	0.74
46	1.72	0.020	0.85	0.99
47	1.72	0.020	0.89	1.03
49	2.72	0.016	0.96	0.88
47	1.74	0.016	0.89	1.28
37	1.24	0.016	0.59	1.19
36	1.24	0.016	0.56	1.13
29	1.00	0.016	0.41	1.02
46	1.72	0.016	0.85	1.26
47	1.72	0.016	0.89	1.29
17	0.55	0.020	0.21	0.74
33	1.00	0.016	0.49	1.22
45	2.20	0.016	0.82	0.93
36	1.24	0.016	0.56	1.13
<u>PEEK-150. $D_p = 17$</u>				
51	5.4	0.010	1.04	0.83
66	4.8	0.016	1.94	1.10
45	4.8	0.010	0.82	0.74
<u>PMR-15. $D_p = 1.5$</u>				
52	7.3	0.020	1.08	0.99
22	3.6	0.010	0.28	1.04

Table 2

Electrostatic Deposition Data LARC-TPI 2000 on AS-4 Carbon Fiber Tows

Tow K	Air Flow Rate, CFH	Voltage kV	Tow Rate U_t cm/sec	Cloud Density n g/cc	Weight Percent P
Ionizer Air Flow Rate Tests					
12	50	75	0.87	0.0015	7
12	100	75	0.87	0.0015	35
3	100	75	1.12	0.0008	9
3	150	75	1.12	0.0008	18
3	100	75	3.85	0.0017	6
3	150	75	3.85	0.0017	12
Discharge Voltage Tests					
12	150	75	0.87	0.0015	35
12	150	0	0.87	0.0015	15
12	150	0	0.87	0.0007	3
12	150	30	0.87	0.0007	3
12	150	50	0.87	0.0007	3
12	150	75	0.87	0.0007	15
12	150	79	0.87	0.0007	15
3	150	0	1.12	0.0015	18
3	150	75	1.12	0.0015	29
Tow Speed Tests					
3	150	75	1.12	0.0016	29
3	150	75	2.56	0.0016	17
3	150	75	0.83	0.0016	40
3	150	75	3.33	0.0016	12
3	150	75	2.04	0.0023	28
3	150	75	0.83	0.0023	44
3	150	75	2.70	0.0023	19

Table 3

Flexural Rigidity of Towpreg LARC-TPI 1500 on 3K Carbon Fiber Tow

Oven Temperature °C	Oven Residence Time Seconds	Weight Percent Resin	Resin Wt Per Area mg/cm ² (b = 0.5 cm)	Overhang (41.5°) cm	Flexural Rigidity mg-cm
395	3.1	23	5.38	53.3	100,000
375	3.1	28	5.77	35.0	31,000
395	5.5	32	6.16	60.0	166,000
375	5.5	33	6.29	42.5	60,000
355	3.1	29	5.90	35.0	32,000
355	3.1	26	5.63	45.0	64,000
355	3.1	26	5.37	40.0	43,000
395	3.1	27	5.76	55.0	120,000
395	3.1	27	5.76	55.0	120,000
375	2.5	22	5.37	17.5	4,000
375	2.5	16	4.98	15.0	*2,100
375	7.5	72	14.93	60.0	400,000
375	4.3	50	8.38	50.0	130,000
375	3.1	24	5.50	40.0	44,000
395	2.5	30	6.03	27.5	15,700
395	2.5	22	5.37	25.0	10,500
395	2.5	29	5.90	25.0	11,500
395	3.1	24	5.50	32.5	23,600
395	4.3	26	5.63	35.0	30,100
375	4.3	33	6.29	35.0	33,700
375	3.1	24	5.50	31.3	21,000
375	2.5	30	6.03	22.5	8,600
415	3.1	33	6.16	36.3	36,800
415	3.1	35	6.42	36.3	38,400
415	3.1	37	6.68	37.5	44,000
395	4.3	39	6.81	41.3	60,000
415	4.2	46	7.72	60.0	208,000
415	4.2	47	7.86	52.5	142,000
355	6.8	39	6.81	65.0	233,000
355	4.2	47	7.86	37.5	52,000
355	3.1	36	6.65	40.0	52,000
355	2.5	29	5.90	15.0	*2,500
375	4.2	46	7.72	50.0	120,000
355	4.2	42	7.20	35.0	47,000

*Powder was not adequately fused to the fiber.

Table 4
Rigidity Data Summary

Oven Temperature °C	355	375	395	415
Time Seconds				
2.5	[29; 2500]*	[30; 8600] [22; 4000] [16; 2100]*	[27; 12600]3	
3.1	[36; 52000] [27; 46300]3	[25; 32000]3	[25; 91000]4	[35; 40000]3
4.2	[45; 50000]2	[48; 125000]2 [33; 33700]	[33; 45000]2	[46; 175000]2
5.5		[33; 60000]	[32; 166000]	
6.8	[39; 233000]			
7.5		[72; 400000]		

Where: [wt % resin; flexural rigidity, mg-cm] number of samples averaged

*Powder was not adequately fused to fiber

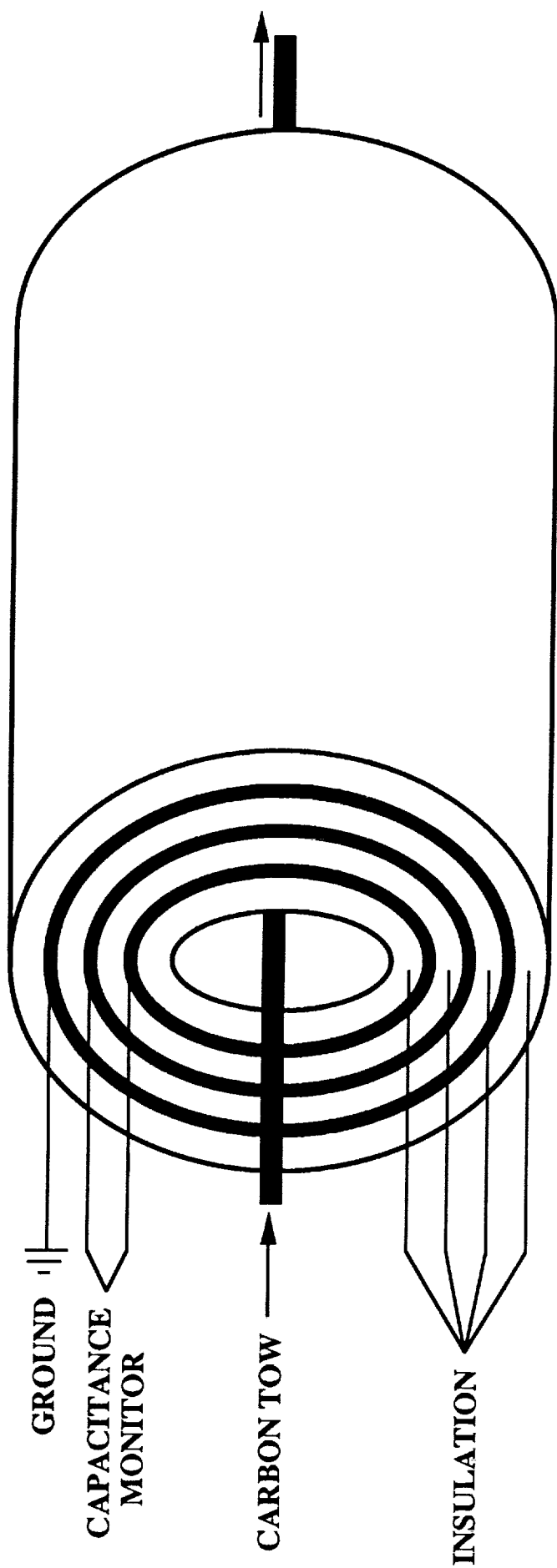


FIGURE 1. SCHEMATIC OF CAPACITOR GAUGE

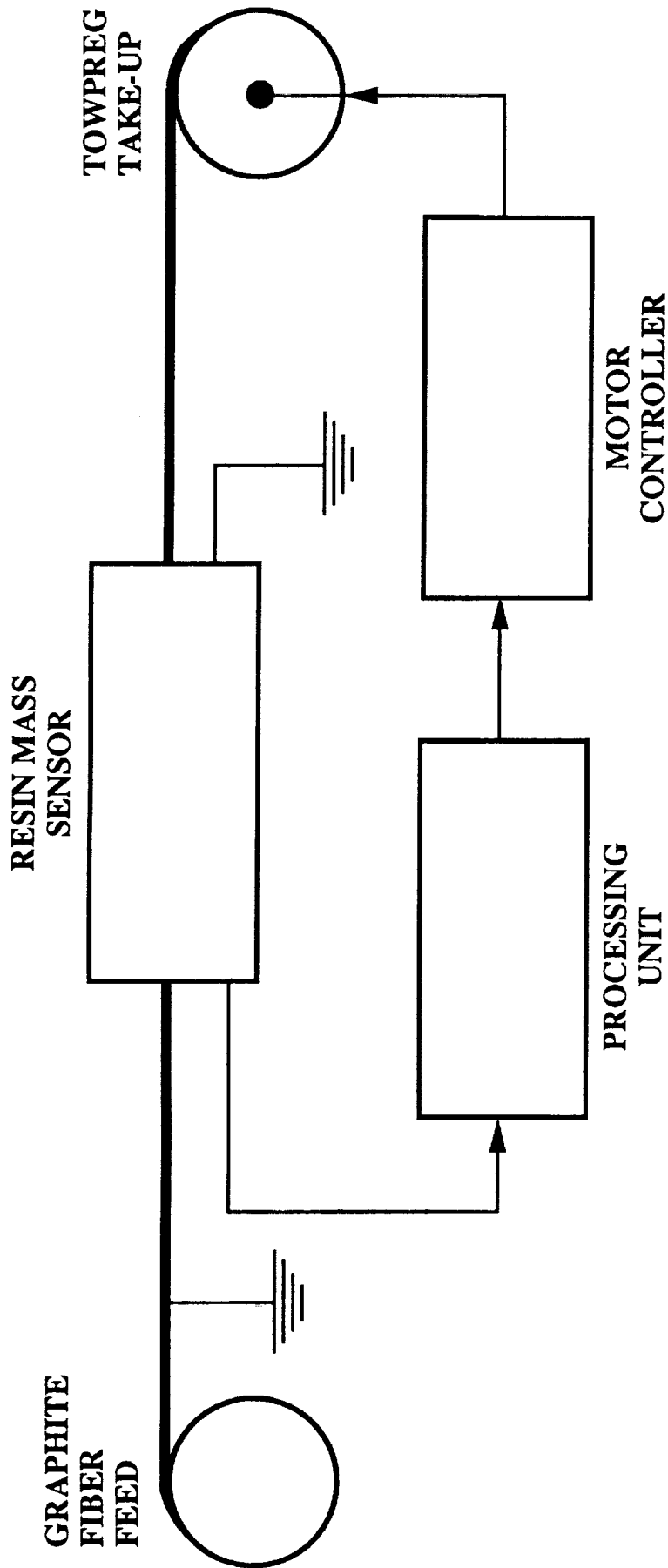
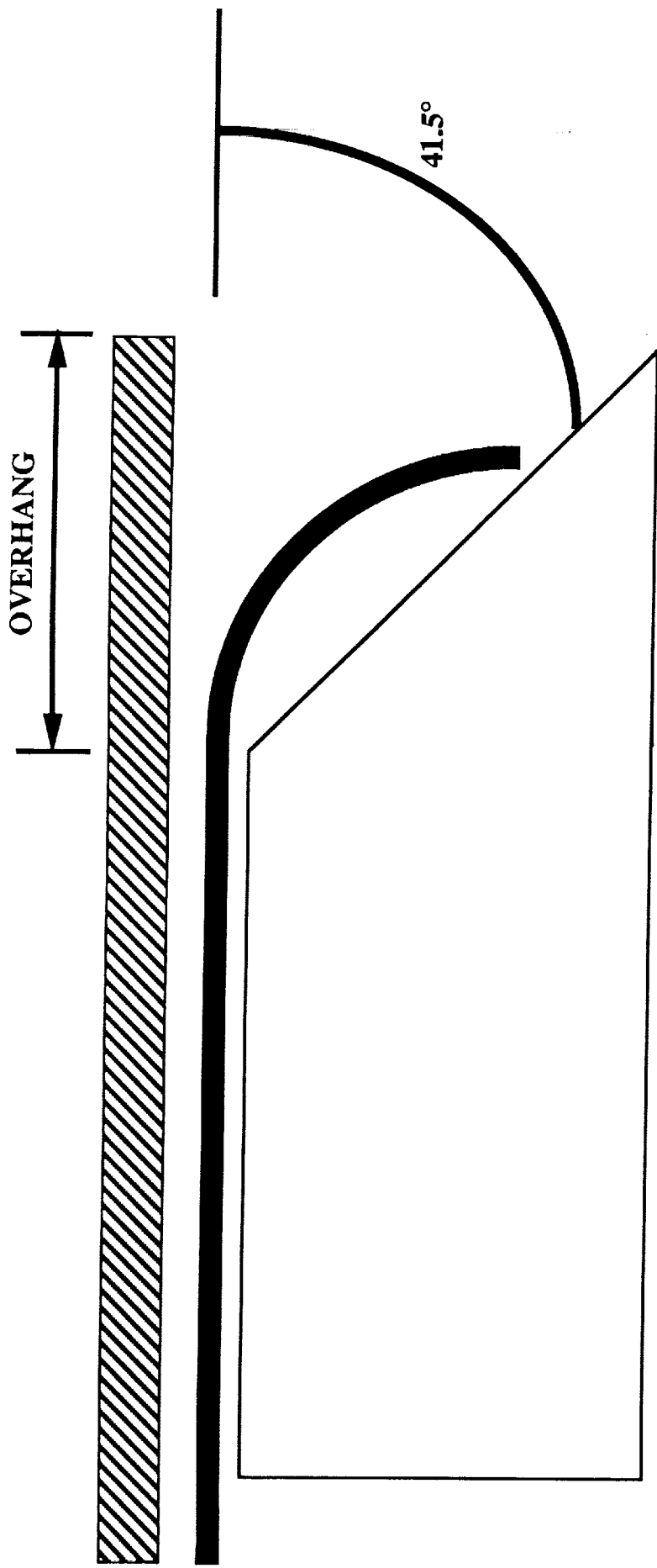


FIGURE 2. SCHEMATIC DIAGRAM OF RESIN MASS MONITOR/TOW SPEED CONTROLLER

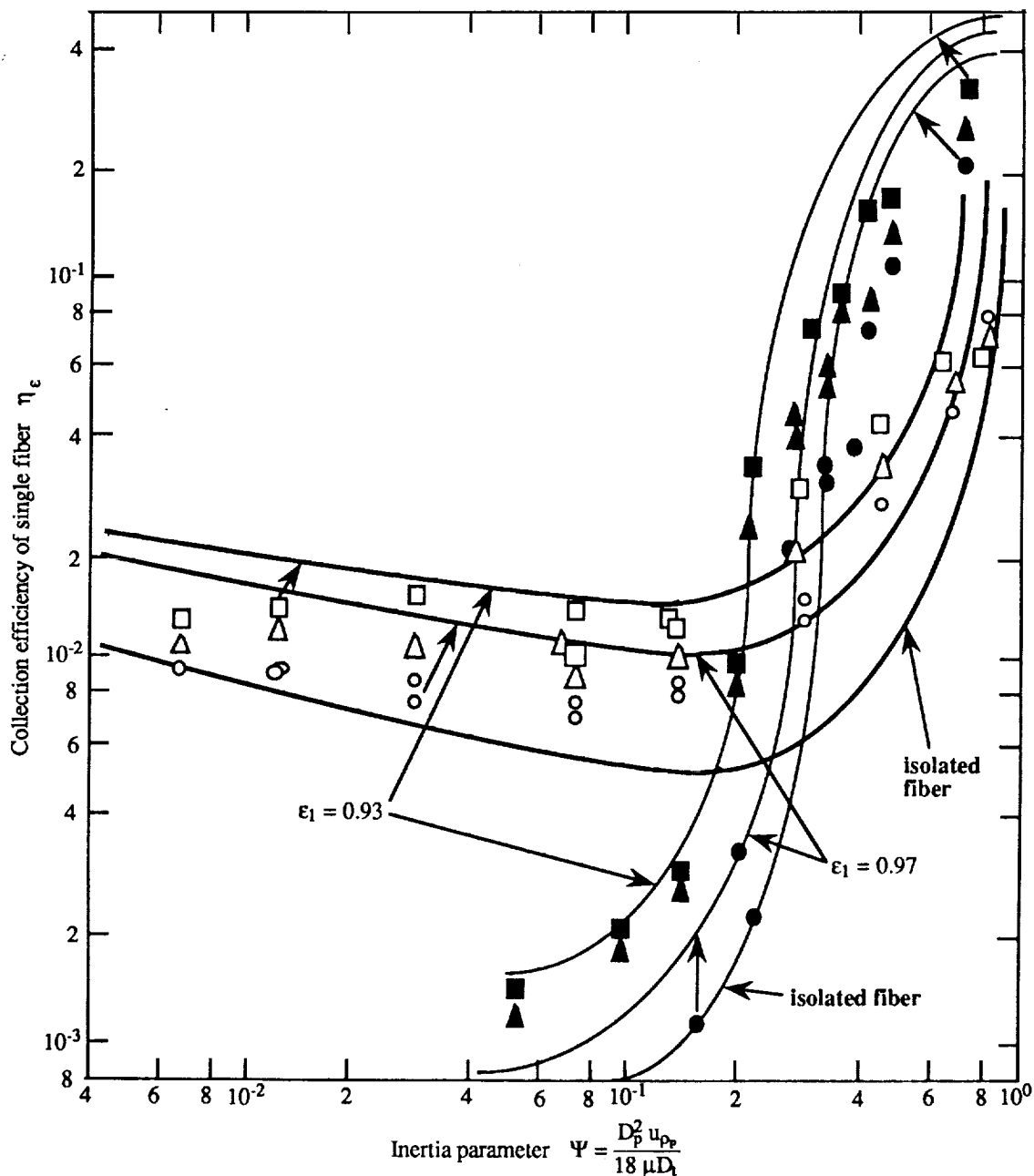


W = WEIGHT PER UNIT AREA (MG/CM²)

O = OVERHANG LENGTH (CM)

G = FLEXURAL RIGIDITY = $W \times (O / 2)^3$ (MG-CM)

FIGURE 3. FLEXURAL RIGIDITY TEST



Theoretical initial collection efficiency of an isolated fiber compared with experimental results (62a). Values for η_ϵ and Ψ are dimensionless; $D_p = 1.0 \mu\text{m}$; bold line: $D_t = 10.46 \mu\text{m}$; normal line: $D_t = 31.9 \mu\text{m}$.

$D_t = 10.46 \mu\text{m}$		$D_t = 31.9 \mu\text{m}$	
Symbol	$1 - \epsilon_1$	Symbol	$1 - \epsilon_1$
○	0.03	●	0.0252
□	0.05	■	0.05
△	0.07	▲	0.07

Reference: Air Pollution, Vol. IV, A. C. Stern, Ed., p 168, Academic Press, 1977.

FIGURE 4. FIBER COLLECTION EFFICIENCY

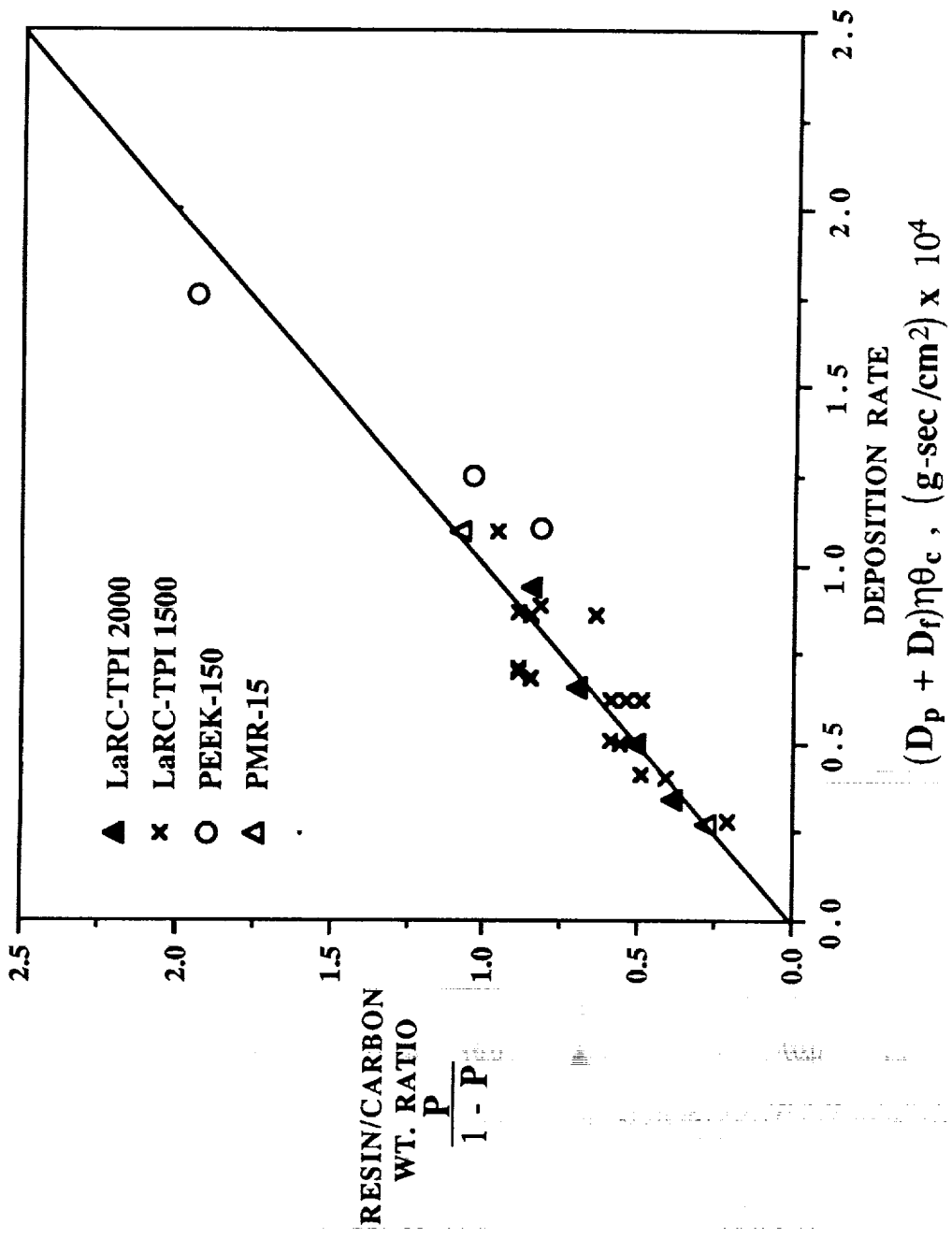

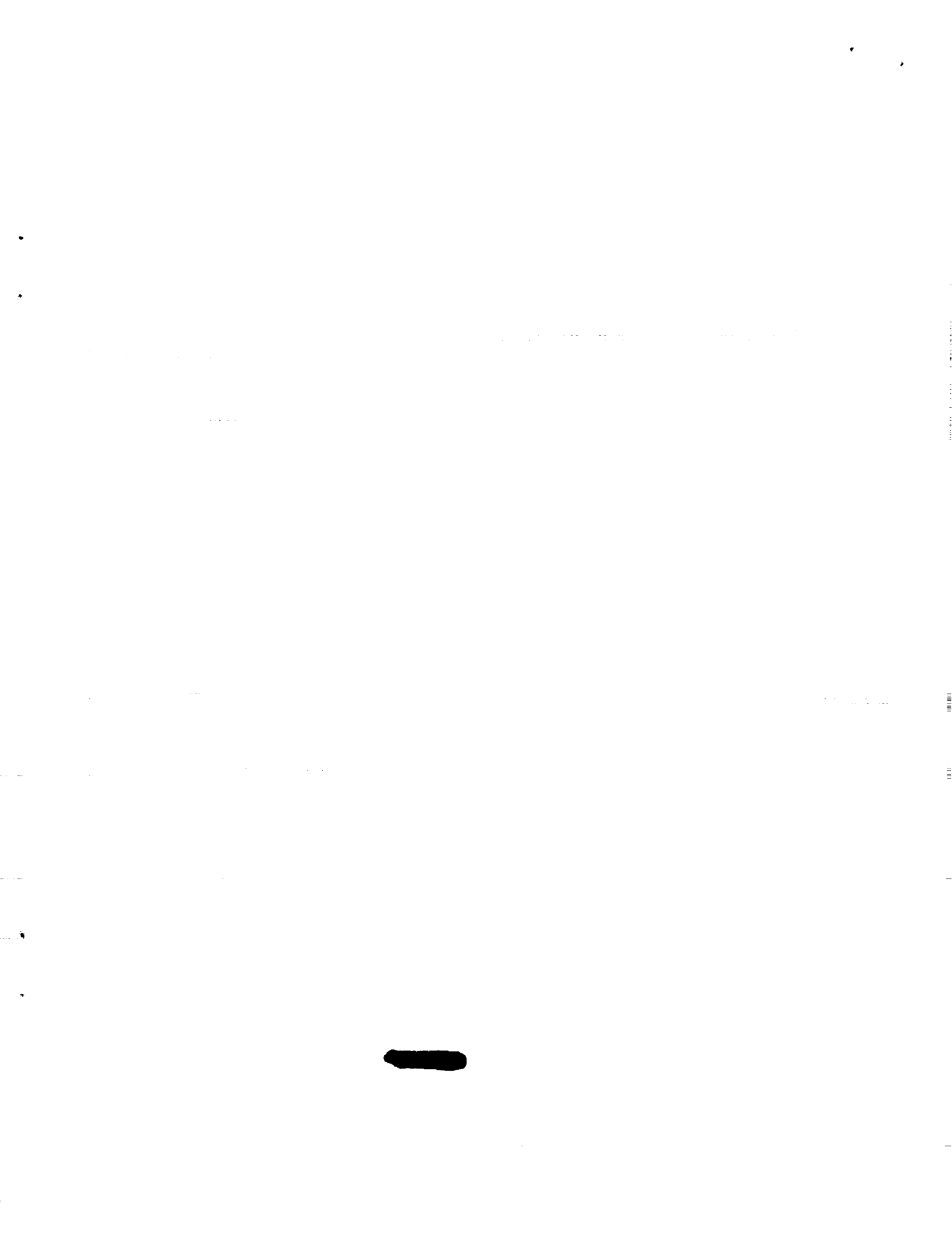


FIGURE 5. POWDER DEPOSITION DATA CORRELATION



Report Documentation Page

1. Report No. NASA TM-102648		2. Government Accession No.		3. Recipient's Catalog No.	
4. Title and Subtitle LaRC Dry Powder Towpreg System			5. Report Date April 1990		
			6. Performing Organization Code		
7. Author(s) Robert M. Baucom and Joseph M. Marchello			8. Performing Organization Report No.		
			10. Work Unit No. 505-63-01-01		
9. Performing Organization Name and Address NASA Langley Research Center Hampton, VA 23665-5225			11. Contract or Grant No.		
			13. Type of Report and Period Covered Technical Memorandum		
12. Sponsoring Agency Name and Address National Aeronautics and Space Administration Washington, DC 20546-0001			14. Sponsoring Agency Code		
			15. Supplementary Notes		
16. Abstract <p>Dry powder polymer impregnated carbon fiber tows have been produced for preform weaving and composite materials molding applications. In the process, fluidized powder is deposited on spread tow bundles and melted on the fibers by radiant heating to adhere the polymer to the fiber.</p> <p>Unit design theory and operating correlations have been developed to provide the basis for scale up of the process to commercial operation. Special features of the operation are the pneumatic tow spreader, fluidized bed, resin feeder, and quality control system.</p> <p>Bench scale experiments, at tow speeds up to 50 cm/sec, have demonstrated that process variables can be controlled to produce weavable LARC-TPI carbon fiber towpreg. The towpreg made by the dry powder process has been formed into unidirectional fiber moldings and has been woven and molded into preform material of good quality.</p>					
17. Key Words (Suggested by Author(s)) Prepregging Dry polymer powder coating Powder coated towpreg			18. Distribution Statement  Subject Category - 24		
19. Security Classif. (of this report) Unclassified		20. Security Classif. (of this page) Unclassified		21. No. of pages 49	22. Price



11

